

## Article

# Impacts of the tropical Pacific–Indian Ocean associated mode on Madden–Julian Oscillation over the Maritime Continent in winter

Xin Li <sup>1,2</sup>, Ming Yin <sup>3</sup>, Xiong Chen <sup>1\*</sup>, Minghao Yang <sup>1</sup>, Fei Xia <sup>1</sup>, and Guangchao Chen <sup>1</sup>,  
Lifeng Li <sup>1</sup>, Peilong Yu <sup>1</sup>, Chao Zhang <sup>1</sup>

<sup>1</sup> College of Meteorology and Oceanography, National University of Defense Technology, Nanjing 211101, China; lixin\_atocean@sina.cn (X.L.); ymhnj@icloud.com (M.Y.); xiafei18@nudt.edu.c; ypl\_cli@sina.cn (P.Y.)

<sup>2</sup> State Key Laboratory of Numerical Modeling for Atmospheric Sciences and Geophysical Fluid Dynamics (LASG), Institute of Atmospheric Physics, Chinese Academy of Sciences, Beijing 100029, China;

<sup>3</sup> Army 32021 of PLA, Beijing 100049, China; ymeffie@163.com (M.Y.)

\* Correspondence: chenx\_dw\_mail@sina.com (X.C.)

**Abstract:** Based on the observation and reanalysis data, the relationship between Madden–Julian Oscillation (MJO) over the Maritime Continent (MC) and the tropical Pacific–Indian Ocean temperature anomaly mode is analyzed. The results showed that the MJO over the MC region (100°–140°E, 10°S–5°N) (referred to as MC–MJO) possesses prominent interannual and interdecadal variations and seasonally "phase-locked" features. MC–MJO is strongest in the boreal winter and weakest in the boreal summer. Winter MC–MJO kinetic energy variation has significant relationships with the El Niño–Southern Oscillation (ENSO) in winter and the Indian Ocean Dipole (IOD) in autumn, but it correlates better with the tropical Pacific–Indian Ocean associated mode (PIOAM). The correlation coefficient between the winter MC–MJO kinetic energy index and the autumn PIOAM index is as high as -0.43. This means that when the positive (negative) autumn PIOAM anomaly strengthens, the MJO kinetic energy over the winter MC region weakens (strengthens). However, the correlation between the MC–MJO convection and PIOAM in winter is significantly weaker. The propagation of MJO over the Maritime Continent differs significantly in the contrast phases of PIOAM. During the positive phase of the PIOAM, the eastward propagation of the winter MJO kinetic energy always fails to move across the MC region and cannot enter the western Pacific. However, during the negative phase of the PIOAM, the anomalies of MJO kinetic energy over the MC is not significantly. MJO can propagate farther eastward and enter the western Pacific. One thing must be pointed out that there is a significant difference between the propagation of MJO convection over the MC region in winter and that of the MJO kinetic energy. That said, the MJO convection is more likely to extend to the western Pacific in the positive phases of PIOAM than in the negative phases.

**Keywords:** the tropical Pacific–Indian Ocean associated mode (PIOAM); Madden Julian Oscillations (MJO); Maritime Continent (MC); MJO kinetic energy; MJO convection

## 1. Introduction

The tropical Pacific and Indian Ocean exhibit the most significant interannual variations of the sea surface temperature (SST) on a global scale and play a critical role in modulating the interannual variations of the global climate, especially in Asia. The El Niño–Southern Oscillation (ENSO) is the dominant component of the interannual variability in the tropical Pacific, while the Indian Ocean

Dipole (IOD) is the most famous interannual variability in the tropical Indian Ocean. In the early stage, they were studied independently. However, more and more researches show that there are strong interactions between the tropical Pacific and Indian Ocean, so that ENSO and IOD should be considered as a whole. Based on this idea, researchers analyzed the Pacific-Indian Ocean SST anomaly by using EOF decomposition. The first mode shows that when the equatorial central-eastern Pacific and tropical central-western Indian Ocean are abnormally warmer (colder), the equatorial western Pacific and eastern Indian Ocean are correspondingly colder (warmer), and this mode is recognized as the Pacific-Indian Ocean associated mode (PIOAM) (Ju et al., 2004; Yang and Li, 2005).

The discovery of the PIOAM has received wide attention, and its characteristics, evolution, and mechanism are preliminarily discussed in the following researches (Wu et al., 2009; Li et al., 2013; Li et al., 2020). It is further pointed out that, the PIOAM in the subsurface is more prominent than that at the surface and it can better reflect the opposite zonal variation of the tropical SSTA. The PIOAM also plays a crucial role in climate anomaly. Yang and Li et al. (2005) studied the influences of the PIOAM on the South Asian High (SAH) and regional climate change (Yang et al., 2006; Li et al., 2018). These influences are quite different from that of the conditions when ENSO and the IOD are discussed separately (Li et al., 2018). However, the investigations above mainly focus on the climatic impacts of the PIOAM in the extra equatorial region on the interannual scale, and the influences of the PIOAM in the equatorial region on the intraseasonal scale remain to be investigated.

The intraseasonal oscillation (ISO) dominates the intraseasonal variability in the tropical atmosphere. The ISO near the equator is also called Madden-Julian Oscillation (MJO; Madden and Julian, 1971, 1972). Many researches indicate that the MJO has direct relationships with the monthly and seasonal climate changes (such as Li et al., 2001; Hall et al., 2001; Donald et al., 2006; Zhang et al., 2009; Bai et al., 2011; Lv et al., 2012), and it is the bridge connecting weather and climate variations (Zhang, 2013).

Previous studies showed that the warm and cold phases of ENSO affect the MJO activity significantly (Li and Zhou, 1994; Li and Smith, 1995; Kessler, 2001; Tam and Lau, 2005; Pohl and Matthews, 2007; Chen et al., 2015), and the impacts of different types of El Niño are also different (Gushchina, et al., 2012; Yuan et al., 2013; Chen et al., 2016; Pang et al., 2016). According to recent observations and simulations, the IOD has significant impacts on the intensity and propagation of the MJO (Wilson et al., 2013; Yuan et al., 2014; Benedict et al., 2015; Seiki et al., 2015), and its influence is even more important than that of ENSO. Considering that the PIOAM is the reflection of the Pacific-Indian Ocean temperature characteristics as a whole, which includes both ENSO signal and the IOD signal. Its influence on the MJO activity over the MC region is probably more significant than either of these two separate components. Based on the above considerations, this paper will discuss the relationships between the PIOAM and the MJO activity over the MC region (MC-MJO), including the impacts of the PIOAM on the intensity, propagation, and structure of the MC-MJO. This paper is arranged into seven sections. In section 2, the data and methods of analysis adopted in this study are described. The differences of the MC-MJO intensity, propagation, and structure between positive and negative PIOAM phases are presented in sections 3 to 5, respectively. Possible causes are given in section 6. The discussion and conclusions make up the final section.

## 2. Data and methods

The reanalysis data used in this paper include the daily atmospheric circulation from the National Center for Environmental Prediction/National Center for Atmospheric Research (NCEP/NCAR) with a horizontal resolution of  $2.5^\circ \times 2.5^\circ$  and from the European Centre for Medium-Range Weather Forecasts Interim Re-Analysis (ERA-Interim; Dee et al., 2011) with the same resolution. These two types of data are adopted to better verify our conclusions. Daily outgoing longwave radiation (OLR) with a horizontal resolution of  $2.5^\circ \times 2.5^\circ$  are also utilized. The monthly sea surface temperature (SST) data are from UK's Hadley Centre for Climate Prediction and Research, with the resolution of  $1.0^\circ \times 1.0^\circ$ . SST and wind cover the period January 1951 to December 2011, and the OLR data are from June 1974 to December 2011.

The MJO signal was obtained using a 30-90 day Lanczos band-pass filter, and in this paper the surface PIOAM associated mode index (SAMI) described by Yang and Li (2005) was calculated using the HadISST data. Anomalous PIOAM years are defined as the autumn SAMI exceeding  $\pm 1.0$  standard deviations. Based on this criterion, seven positive phase years (1982, 1986, 1987, 1994, 1997, 2002, 2006) and six negative years (1988, 1996, 1998, 2005, 2007, 2010) are identified. The Maritime Continent (MC) is described as the area within  $15^{\circ}\text{S}$ - $5^{\circ}\text{N}$ ,  $100^{\circ}$ - $140^{\circ}\text{E}$ . The MJO kinetic energy intensity index over the MC region is defined as the standard deviation of the regional averaged MJO zonal wind with the climatological mean removed. Index values greater than 1.0 standard deviation are selected as strong MJO kinetic energy intensity cases, and index values less than -1.0 standard deviation are chosen as weak MJO kinetic energy intensity cases.

### 3. Differences of MJO intensity over the MC between positive and negative phases of PIOAM

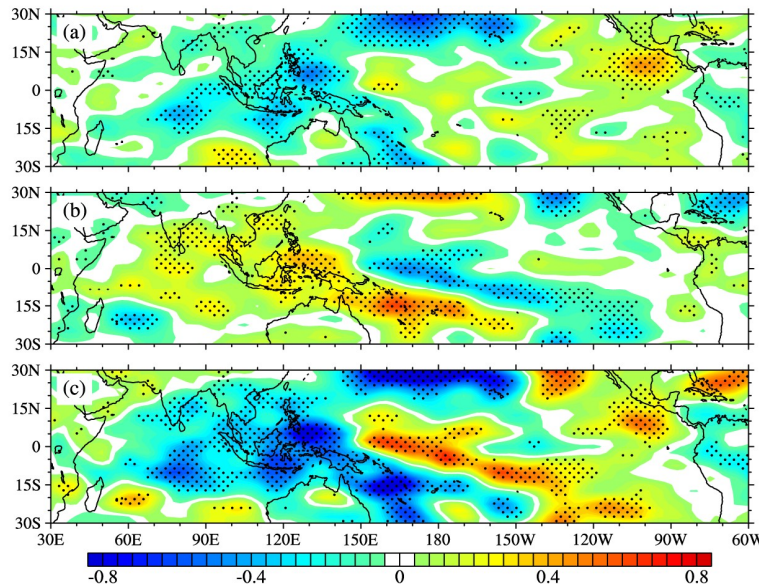
MJO intensity is one of the important characteristics of the MJO activity, and it is usually described by the MJO kinetic energy and OLR amplitude. The procedure for calculating the MJO signal  $\tilde{f}$  is as follows (Yuan et al., 2015): (1) remove the climatological mean of the daily grid data  $f$ ; (2) obtain the MJO signal  $\tilde{f}$  by adopting a 30-90 day Lanczos band-pass filter. The MJO kinetic energy is calculated using the following formula:

$$\tilde{E}_f = 1/2\tilde{f}^2. \quad (1)$$

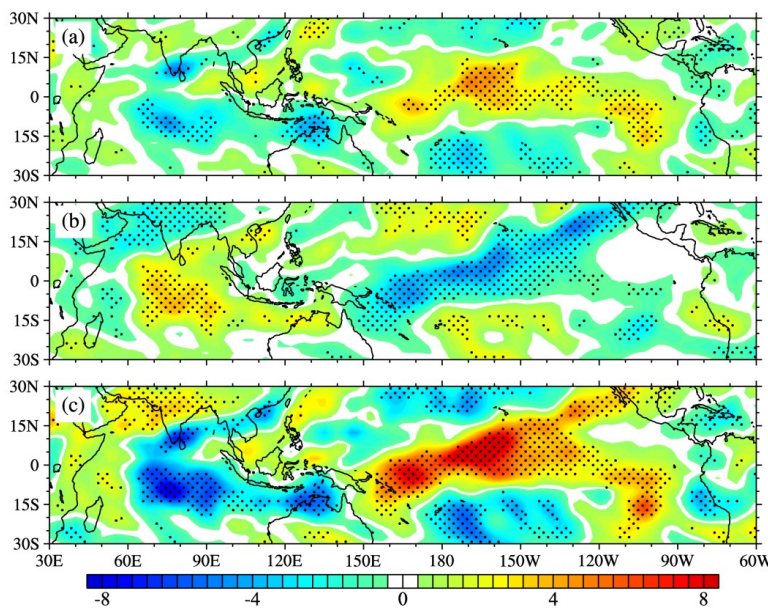
In this paper,  $f$  refers to zonal wind at 850hPa. The MJO OLR amplitude is defined as follows:

$$A_f = \tilde{f}^2, \quad (2)$$

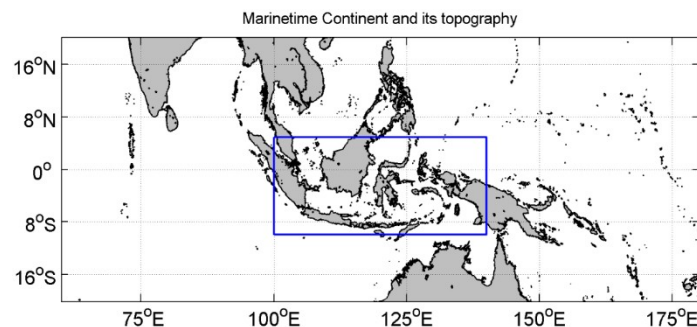
where  $f$  is OLR. Composite MJO kinetic energy in autumn and winter, spring, and summer between the positive and negative phases of the PIOAM are conducted chronologically and the results indicate that the largest differences occur in winter. Thus, this paper mainly focuses on the MJO activity in winter in the positive and negative phases of the PIOAM. Composite MJO kinetic energy in the positive and negative phases of the PIOAM (Figure 1) shows that the MJO kinetic energy over the equatorial eastern Indian Ocean and the Maritime Continent is significantly weakened in the positive phase years. They are significantly enhanced over the equatorial eastern Indian Ocean, the Maritime Continent, and Australia's northeast coast in negative phase years, and the MJO kinetic energy decreases significantly over the equatorial western Pacific and central-southern Pacific. It is obvious that there are prominent differences in the MJO intensity between positive and negative phases of the PIOAM, especially over the Maritime Continent. In contrast, the differences in MJO OLR amplitudes between positive and negative PIOAM phases are far less significant than that of MJO kinetic energy, and they show a seesaw pattern in meridional direction (Figure 2). Similar results are acquired when correlation analyses of the PIOAM index with the MJO kinetic energy and OLR amplitude are carried out (Figure omitted). These results indicate that, to some extent, there are significant differences between the MJO activity and the MJO convection, and the causes will be analyzed in another paper. Here, we focus on the relationships between the PIOAM and the MJO activity in winter over the MC region. The center of MJO activity is mainly over the southern hemisphere so that we define the MC region as the  $10^{\circ}\text{S}$ - $5^{\circ}\text{N}$ ,  $100^{\circ}$ - $140^{\circ}\text{E}$  (Figure 3). MJO kinetic energy index is presented as the MJO kinetic energy averaged over the MC region. The yearly evolution of MJO kinetic energy index (Figure 4) shows that besides interannual variation, the MJO kinetic energy in winter also exhibits significantly interdecadal variation. It enhanced notably in the middle and late 1950s, the early and middle 1970s, the middle 1980s to the early 1990s, and the early and middle 2000s, while it weakened remarkably in the 1960s, the late 1970s to the early 1980s and the middle 1990s to the early 2000s.



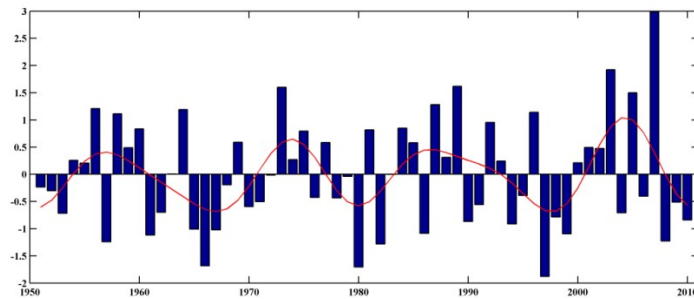
**Figure 1.** Composite anomalous MJO zonal wind amplitude at 850 hPa ( $\text{m} \cdot \text{s}^{-1}$ ) during the (a) positive and (b) negative phases of the PIOAM, and (c) their difference (positive minus negative). Results passing the significant test at the 90% confidence level are stippled.



**Figure 2.** As in Figure 1, but for the anomalous MJO OLR amplitude ( $\text{w} \cdot \text{m}^{-2}$ )

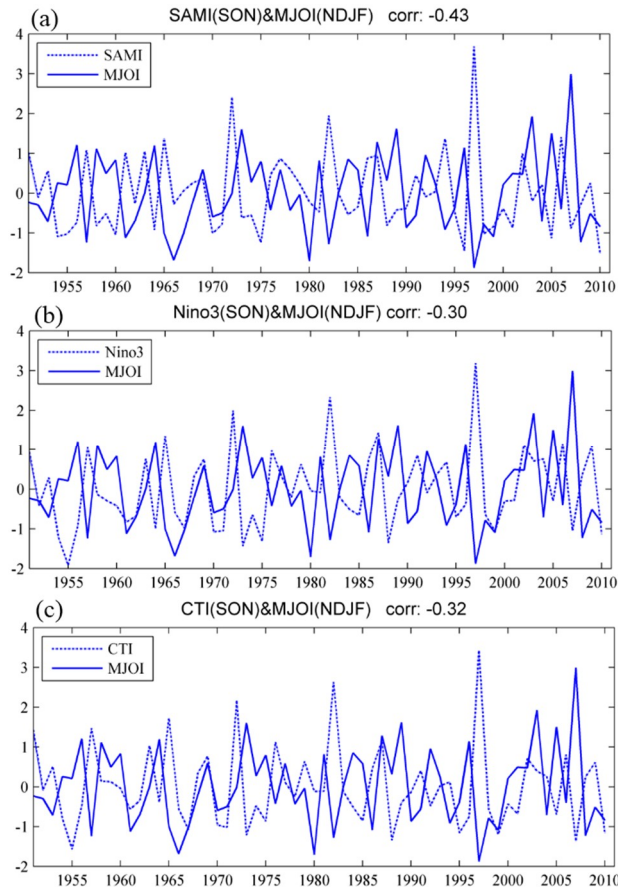


**Figure 3.** The terrain of the Maritime Continent (blue rectangle) and adjacent areas.



**Figure 4.** Yearly MC-MJO kinetic energy index in winter (bar). Results after nine point low pass filter are given in the red dashed line.

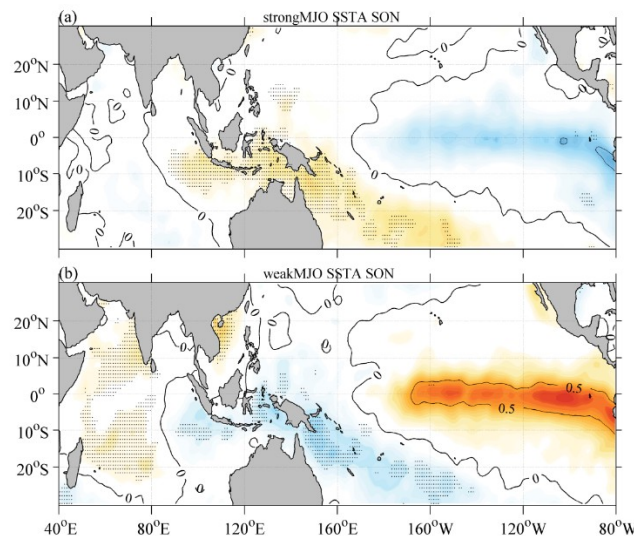
Correlations between the winter (November to February in the following year) MJO kinetic energy index and the SAMI in summer (June to August), autumn (September to November), winter (December to February in the following year) are calculated respectively. Results show that the autumn SAMI has the best correlation with the winter MJO index. The coefficient is as high as -0.43, which exceeds significant test at 99% confidence level. That means when the positive autumn PIOAM anomaly strengthens, the MJO kinetic energy over the winter MC region enhances, and vice versa. On the other hand, the MC-MJO kinetic energy index has weaker correlations with the Niño 3 index and Cold Tongue Index (CTI). The above analyses revealed that the PIOAM has more important impacts on the winter MJO activity over the MC region than the El Niño.



**Figure 5.** Correlation coefficients of the winter MC-MJO index with the autumn (a) SAMI, (b) Nino3 index, and (c) CTI.

Strong and weak MC-MJO winters are defined as the MJOI exceeding one standard deviation. Ten strong cases (1956, 1958, 1964, 1973, 1987, 1989, 1996, 2003, 2005, 2007) and eleven weak cases (1957, 1961, 1965, 1966, 1967, 1980, 1982, 1986, 1997, 1999, 2008) are selected. Composite autumn SST

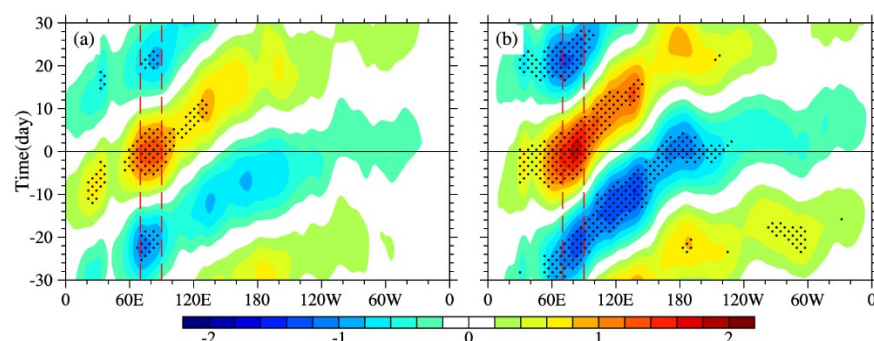
in the strong and weak MC-MJO cases are shown in Figure 6. In strong MC-MJO cases, the equatorial southeastern Indian Ocean and tropical southwestern Pacific are significantly warmer, while the western Indian Ocean and eastern Pacific are slightly colder. This pattern is similar to the negative phase of the PIOAM (Figure 6a). On the contrary, in the weak MC-MJO cases, the equatorial southeastern Indian Ocean and tropical southwestern Pacific are significantly colder, while the western Indian Ocean and eastern Pacific are significantly warmer. The feature conforms to the positive phase of the PIOAM (Figure 6b). The above researches suggest again that there are good correlations between the intensity of the MJO kinetic energy over the MC region and the PIOAM.



**Figure 6.** Composite distribution of SST ( $^{\circ}$ C) in autumn during the (a) strong and (b) weak MC-MJO cases.

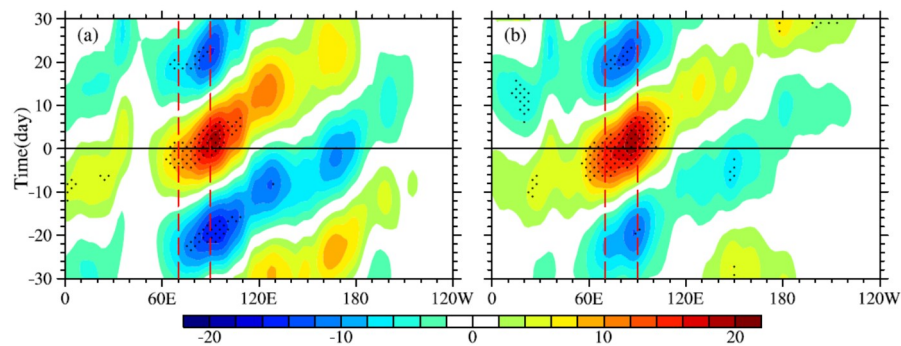
#### 4. Differences of the eastward propagation of MJO between positive and negative phases of PIOAM

The eastward propagation of MJO kinetic energy along the equator is an important feature of MJO activity, which contributes to the initiation and eastward expansion of the equatorial westerly anomaly. Figure 7 shows MJO zonal winds at 850 hPa averaged over the 10°S-10°N lag regressed onto that averaged over the 10°S-10°N, 70°-90°E in positive and negative PIOAM phases. In the winter of the negative phase of the PIOAM, the MJO activity is significantly stronger, consistent with the results of composite analysis and correlation analysis. Accordingly, the eastward propagation of the MJO is more prominent, and it can propagate even to the dateline. In the winter of the positive phase of the PIOAM, the MJO kinetic energy over the MC region is noticeably weaker. As a result, its eastward propagation is also significantly weaker and MJO generally is confined to the east of the Maritime Continent.



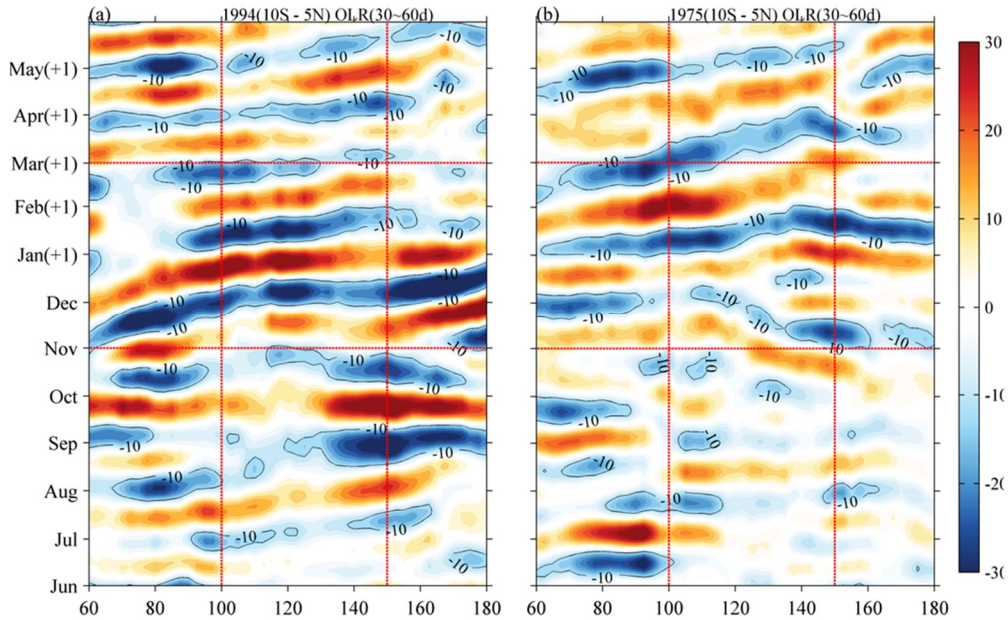
**Figure 7.** Longitude-time diagram of the MJO zonal winds at 850 hPa averaged over the 10°S-10°N lag regressed onto that averaged over the 10°S-10°N, 70°-90°E during the (a) positive and (b) negative phases of PIOAM. Results passing the significant test at the 90% confidence level are stippled.

Figure 8 shows the regressed MJO OLR averaged over the 10°S-10°N at 850 hPa onto the 30-90 day Lanczos band-pass filtered OLR averaged over the 10°S-10°N, 70°-90°E. During the positive phase of the PIOAM, the MJO convection over the equatorial eastern Indian Ocean (corresponding to the third phase of the MJO) is weaker than that during the negative phase, while the MJO convection is stronger over the Maritime Continent and equatorial western Pacific (corresponding to the fourth and fifth phases of the MJO) than that during the negative phase. This means the MJO can propagate farther east in the positive PIOAM phase, and the character is different from that of the propagation of the MJO kinetic energy, which indicates that the MJO kinetic energy and convection over the MC region are not completely corresponding.



**Figure 8.** Longitude-time diagram of the MJO OLR ( $w \cdot m^{-2}$ ) at 850 hPa averaged over the 10°S-10°N lag regressed onto the 30-90 day Lanczos band-pass filtered OLR averaged over the 10°S-10°N, 70°-90°E at 850 hPa during the (a) positive and (b) negative phases of PIOAM. Results passing the significant test at the 90% confidence level are stippled.

We further take 1994 and 1975 as typical examples for positive and negative PIOAM phases respectively to analyze the practical MJO propagation. The results demonstrate that compared with the condition in the winter (November to February in the following year) of the negative PIOAM phase, more MJO convection can extend to the western Pacific and even farther (Figure 9a, 9b) in the winter of the positive PIOAM phase. The MJO convections in other typical positive and negative phase years (such as 1987 and 1988, 2002 and 2001) are compared and analyzed, and similar conclusions can be obtained (Figure omitted).



**Figure 9.** Longitude-time diagram (colors,  $w \cdot m^{-2}$ ) of the MJO OLR averaged over the  $10^{\circ}\text{S}$ - $5^{\circ}\text{N}$  during the (a) positive and (b) negative phases of PIOAM.

##### 5. Differences of the MJO structure over the Maritime Continent between positive and negative phases of PIOAM

Figure 10 shows the regressed MJO zonal-vertical circulation onto the winter MC-MJO OLR index. There are apparent differences between positive and negative PIOAM phases, especially over the Maritime Continent. In the winter of the positive PIOAM phase, when the MJO extends to the Maritime Continent, the westerly anomalies at the low-level are significantly weaker than that in the negative phase, which corresponds with the above conclusion that the MC-MJO kinetic energy is stronger in the winter of the negative PIOAM phase than that in the positive phase. However, the easterly anomalies at a high level in the positive phase are slightly stronger than that in the negative phase. There are no noticeable differences in the vertical advection over the MC region, which may explain why the MC-MJO OLR has no significant difference in the winter of the positive and negative PIOAM phases.

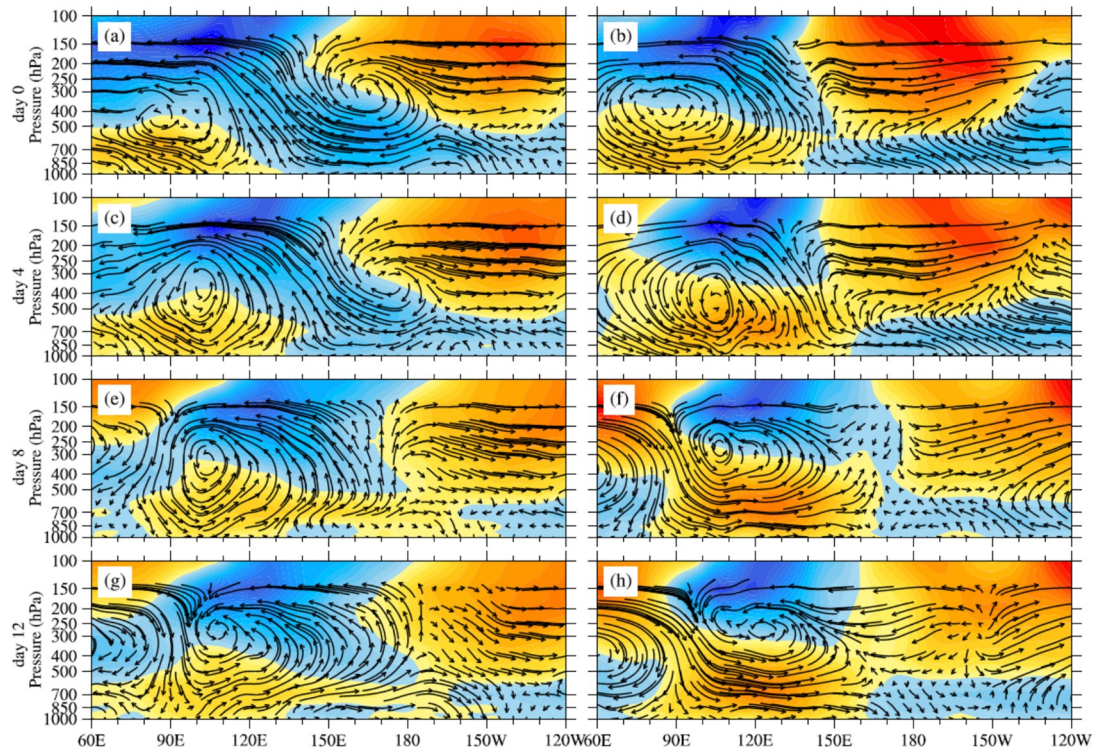


**Figure 10.** MJO zonal vertical circulation (vectors, magnified 100 times in the vertical direction, colors represent vertical velocity) lag regressed onto the MC-MJO OLR index during the positive (left row) and negative (right row) phases of PIOAM.

In the winter of the positive PIOAM phase, when MJO activity passes by over the Maritime Continent, the westerly anomalies at the low-level troposphere slightly strengthen and propagate eastward, but they are far less significant than that in the negative phases. In contrast, in the winter of the positive PIOAM phase, there is strong anomalous ascending motion with significant eastward propagation, while in the negative PIOAM phase, the anomalous ascending motion weakens over time and the eastward propagation is not significant. This shows on the other side that in the negative PIOAM phase, the MC-MJO kinetic energy is stronger and the distance of eastward propagation of MJO is longer than that in the positive PIOAM phase, while the MC-MJO convection is more likely to propagate across the Maritime Continent during the positive phase of the PIOAM.

## 6. Causes for the different characteristics in positive and negative phases of PIOAM

### 6.1 abnormal distribution of SST

Previous studies have revealed that MJO intensity has close relationships with the underlying SST. Composite SSTA in autumn in the anomalous years of PIOAM are shown in Figure 11. In the positive phase of PIOAM, the Indian Ocean exhibits the positive phase of the IOD, while the Pacific presents the strong El Niño pattern with SST dropping significantly over the MC region and adjacent waters and vice versa. Wilson et al. (2013) pointed out that based on analyses in the observational data, the MJO activity is significantly weak (strong) over the Indian Ocean and Maritime Continent during the positive (negative) phase of IOD. Li and Zhou (1994) reported that after the strong El Niño event, MJO activities over the equatorial Indian Ocean and western Pacific are reduced obviously. As a result, during the positive phase of the PIOAM, the coordinated distribution of the positive IOD in the Indian Ocean and El Niño in Pacific excites the reduction of the MJO activity over the Maritime Continent, while the negative IOD phase in the Indian Ocean and the strong La Niña in Pacific favor the enhancement of the MC-MJO activity. Besides, local SSTA may also have influences on the MJO intensity over the MC region. That said, positive SSTA contributes to strengthening the MJO activity, while negative SSTA is not.

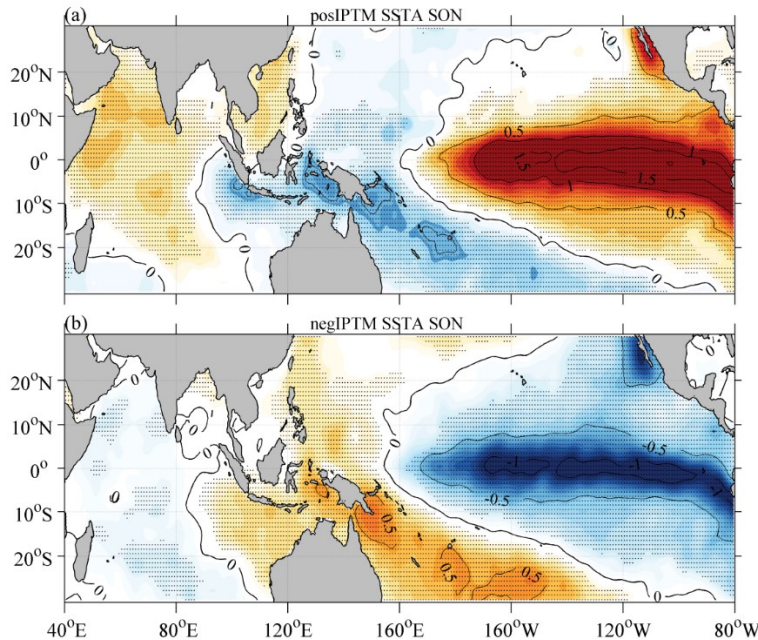


**Figure 11.** Composite SSTAs ( $^{\circ}$ C) in autumn during the (a) positive and (b) negative phases of PIOAM.

#### 6.2 abnormal distribution of horizontal wind field

Many studies have proved that there are connections between the MJO activity and equatorial zonal wind at 850 hPa. Jia (2006) found that tropical intraseasonal oscillation mainly occurs in mean westerlies and weak zonal winds and further pointed out that the impacts of zonal winds may be more important than that of SST. Composite horizontal wind anomalies in winter in the positive and negative phases of the PIOAM are shown in Figure 12. During the winter of the positive PIOAM phase, there is strong easterly anomaly over the equatorial Indian Ocean and Maritime Continent, which weakens the MJO activity over the MC region. During the winter of the negative PIOAM phase, the significant westerly anomaly over the equatorial Indian Ocean and Maritime Continent strengthens the MJO activity over the MC region. Li (2004) reported that the MJO activity also possesses a close association with the East Asian winter monsoon (EAWM) and strong (weak) EAWM excites the enhancement (reduction) of MJO activity over the equatorial western Pacific. Compared with Figure 12a and 12b, EAWM weakens (strengthens) during the positive (negative) PIOAM phase, which may cause the MJO activity over the equatorial western Pacific and Maritime Continent to weaken (strengthen).

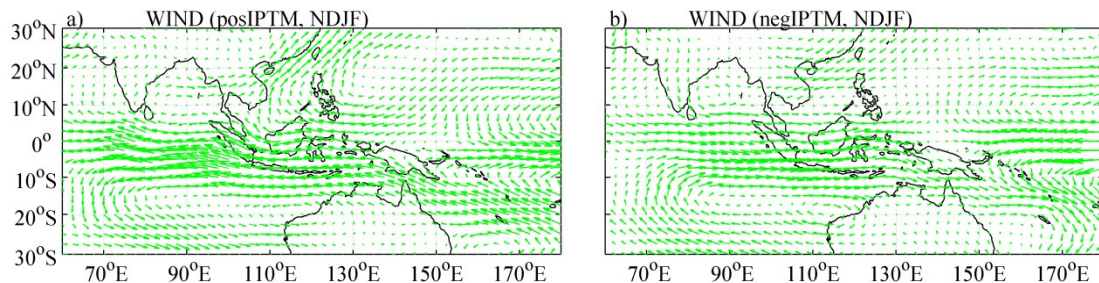


**Figure 12.** Composite horizontal wind field at 850 hPa ( $m \cdot s^{-1}$ ) in winter (November to February in the following year) during (a) positive and (b) negative phases of PIOAM.

#### 7. Conclusions and discussions

Based on the HadISST, NCEP reanalysis data of the atmospheric circulation and OLR datasets, the relationships between the MJO activity in the boreal winter over the Maritime Continent and the PIOAM are examined. The main conclusions are as follows.

(1) MC-MJO possesses prominent seasonally "phase-locked" features which means that the MJO is strongest in the boreal winter and weakest in the boreal summer. MC-MJO also exhibits significant interannual and interdecadal variations.

(2) In winter (November to February in the following year), the interannual variation of the MC-MJO kinetic energy has significant correlations with the winter ENSO and the autumn IOD, but it corresponds better with the PIOAM. When positive (negative) PIOAM anomaly in autumn is stronger (weaker), the MJO kinetic energy over the MC region in winter is lower (higher). However, the MC-MJO convection in winter has no such close association with the PIOAM.

(3) The positive and negative PIOAM phases greatly influences the propagation of the MC-MJO. During the positive phase of the PIOAM, the MJO kinetic energy in winter usually fails to move across the Maritime Continent and arrives into the western Pacific, while during the negative phase of the PIOAM, the MJO kinetic energy over the MC region can propagate to the equatorial western Pacific without significant reduction. In contrast, the preliminary statistical results reveal that the MJO convection during the positive PIOAM phase tends to move across the Maritime Continent and arrive in the equatorial western Pacific more easily than in the negative PIOAM phase, which is not consistent with the propagation of the MC-MJO kinetic energy.

During the positive (negative) phases of the PIOAM in winter, the possible causes for the suppressed (enhanced) MC-MJO activity can be attributed to two reasons. One is the anomalous SSTA pattern and the other is the easterly (westerly) anomaly over the MC region. During the positive (negative) phase of the PIOAM, both the positive (negative) IOD phase in the Indian Ocean and the strong El Niño (La Niña) in Pacific favor the enhancement (reduction) of the MC-MJO activity in winter. Local low (high) SST over the MC region also inhibits (promotes) the development of the MJO activity. On the other hand, during the positive (negative) phase of the PIOAM, the easterly (westerly) anomaly may play a more important role in the reduction (enhancement) of the MJO kinetic energy. Why in the negative PIOAM phase MJO kinetic energy moves across the MC region more easily than in the positive phase of the PIOAM has strong relevance to the fact that MC-MJO kinetic energy is stronger in the negative PIOAM phase than that in the positive phase.

As for the reasons for the inconsistency between the MC-MJO convection and MC-MJO kinetic energy, as well as the mechanism of the convective effective passage rate of the MC-MJO during positive and negative phases of the PIOAM, we will discuss further in the next paper.

**Author Contributions:** Conceptualization, X.L. and X.C.; methodology, X.C.; software, M.Y.; validation, X.L., M.Y. and F.X.; formal analysis, M.Y and C.Z.; investigation, X.L. and F.L.; resources, X.L.; data curation, P.Y. and G.C.; writing—original draft preparation, X.L.; writing—review and editing, X.L. and M.Y.; visualization, X.L. and M. Y.; supervision, X.C. and X.L.; project administration, X.L.; funding acquisition, X.C. and X.L. All authors have read and agreed to the published version of the manuscript.

**Acknowledgments:** This work was supported by the National Natural Science Foundation of China (Grant Nos. 41605051, 41520104008 and 41490642) and Key Research Program of National University of Defense Technology (ZK17-02-010).

**Conflicts of Interest:** The authors declare no conflict of interest.

## References

1. Bai, X., Li, C., Tan, Y., et al. The impacts of the MJO (Madden–Julian Oscillation) on spring rainfall in East China. *J. Trop. Meteor.* (in Chinese), 2011, 27 (6): 814–822.
2. Benedict, J., J., Pritchard, M., S., and Collins, W., D. Sensitivity of MJO propagation to a robust positive Indian Ocean dipole event in the superparameterized CAM. *J. Adv. Model. Earth Syst.*, 2015, 7: 1901–1917.
3. Chen, X., Li, C., and Tan, Y. The influence of El Niño on MJO over the equatorial pacific. *J. Ocean. Univ. China*, 2015, 14: 1–8.
4. Chen, X., Ling, J., and Li, C. Evolution of the Madden–Julian Oscillation in two types of El Niño. *J. Clim.* 2016, 29:1919–1934.

5. Dee, D., and Coauthors, P. The ERA-Interim reanalysis: configuration and performance of the data assimilation system. *Q. J. R. Meteorol. Soc.* 2011, 137: 553–597.
6. Donald, A., Meinke, H., Power, B., A., et al. Near-global impact of the Madden-Julian Oscillation on rainfall. *Geophys. Res. Lett.*, 2006, 33, L09704.
7. Gushchina, D., and Dewitte, B. Intraseasonal tropical atmospheric variability associated with the two flavors of El Niño. *Mon. Wea. Rev.*, 2012, 140: 3669-3681.
8. Hall, J., D., Matthews, A., J., Haroly, D., J. The modulation of tropical cyclone activity in Australian region by the Madden-Julian Oscillation. *Mon. Wea. Rev.*, 2001, 129 (12): 2970-2982.
9. Jia, X. Numerical Simulation of the Intraseasonal Oscillation. Ph. D. dissertation (in Chinese), Graduate University of Chinese Academy of Sciences, 2006.
10. Ju, J., Chen, L., Li, C. The preliminary research of Pacific-Indian Ocean sea surface temperature anomaly mode and the definition of its index. *Journal of Tropical Meteorology* (in chinese), 2004, 20 (6): 617-624.
11. Kessler, W., S. EOF representations of the Madden-Julian Oscillation and its connection with ENSO. *J. Climate*, 2001, 14: 3055-3061.
12. Li, C. New progress in the study of atmospheric Intraseasonal Oscillation. *Advances in Natural Science*, 2004, 14 (07): 15-22.
13. Li, C., and Smith, I. Numerical simulation of the tropical intraseasonal oscillation and the effect of warm SSTs. *Acta Meteor. Sin.*, 1995, 9: 1-12.
14. Li, C., and Zhou, Y. Relationship between Intraseasonal Oscillation in the tropical atmosphere and ENSO. *Acta Geophysica Sinica* (in Chinese), 1994, 37: 17-26.
15. Li, C., Li, X., Yang, H., Pan, J., Li, G. Tropical Pacific-Indian Ocean associated mode and its climatic impacts. *Chinese Journal of Atmospheric Sciences* (in Chinese), 2018, 42 (3): 505–523.
16. Li, C., Li, Z., Zhang, Q. Strong/ weak summer monsoon activity over the South China Sea and atmospheric intraseasonal oscillation. *Adv. Atmos. Sci.*, 2001, 18: 1146-1160.
17. Li, X., Li, C. The tropical Pacific-Indian Ocean associated mode simulated by LICOM2.0. *Adv. Atmos. Sci.*, 2017, 34 (12): 1426-1436.
18. Li, X., Li, C., Tan, Y., Zhang R., and Li, G. Tropical Pacific-Indian Ocean thermocline temperature associated anomaly mode and its evolvement. *Chinese Journal of Geophysics* (in Chinese with English abstract), 2013, 56: 3270-3284.
19. Li, X., Xia, F., Chen, X., Shu, X., Yang, M., Li, L., and Wang, D. The interannual cycle features of the tropical Pacific-Indian Ocean associated mode and its mechanisms. *Journal of Coastal Research*, 2020, 99 (Sp1): 364-372.
20. Lü, J., Ju, J., Ren, J., et al. The influence of the Madden-Julian oscillation activity anomalies on Yunnan's extreme drought of 2009–2010. *Science China: Earth Sciences* (in Chinese), 2012, 55 (1): 98–112.
21. Madden, R. A., and Julian, P., R. Detection of a 40-50 day oscillation in the zonal wind in the tropical Pacific. *J. Atmos. Sci.*, 1971, 28: 702-708.
22. Madden, R. A., Julian, P., R. Description of global-scale circulation cells in the tropics with a 40–50 day period. *J. Atmos. Sci.*, 1972, 29 (6): 1109-1123.
23. Pang, B., Chen, Z., Wen, Z., et al. Impacts of two types of El Niño on the MJO during boreal winter. *Adv. Atmos. Sci.* 2016, 33: 979-986.
24. Pohl, B., and Matthews, A., J. Observed changes in the lifetime and amplitude of the Madden-Julian Oscillation associated with interannual ENSO sea surface temperature anomalies. *J. Climate*, 2007, 20: 2659-2674.
25. Seiki A., Nagura, M., and Hasegawa, T. Seasonal onset of the Madden-Julian oscillation and its relation to the southeastern Indian Ocean cooling. *J. Meteorol. Soc. Jpn.*, 2015, 93(A): 139–156.
26. Tam, C., Y., and Lau, N. C. Modulation of the Madden-Julian Oscillation by ENSO: inferences from observations and GCM simulations. *J. Meteor. Soc. Japan*, 2005, 83: 727-743.
27. Wilson, E., A., Gordon, A., L., and Kim, D. Observations of the Madden Julian oscillation during Indian ocean dipole events. *J. Geophys. Res. Atmos.*, 2013, 118: 2588–2599.
28. Wilson, E., A., Gordon, A., L., and Kim, D. Observations of the Madden Julian Oscillation during Indian Ocean Dipole events. *J. Geophys. Res.*, 2013, 118: 2588–2599.
29. Wu, H., Li, C. The preliminary research of equatorial Pacific-Indian Ocean temperature anomaly mode and subsurface ocean temperature anomalies. *Acta Oceanologica Sinica* (in chinese), 2009, 31 (2): 24-33.

30. Yang, H., Jia, X., Li, C. 2006: The tropical Pacific-Indian Ocean temperature anomaly mode and its effect. *Chin. Sci. Bull. (in Chinese)*, 51 (23): 2878-2884.
31. Yang, H., Li, C. Effect of the Tropical Pacific-Indian Ocean Temperature Anomaly Mode on the South Asia High. *Chinese Journal of Atmospheric Science (in chinese)*, 2005, 29 (1): 99-110.
32. Yuan, Y., Li, C., and Ling, J. Different MJO activities between EP El Niño and CP El Niño (in Chinese). *Scientia Sinica Terra*, 2015, 45: 318-334.
33. Yuan, Y., Li, C., and Ling, J. Different MJO activities between EP El Niño and CP El Niño. *Scientia Sinica Terra* (in Chinese), 2015, 45, 318-334.
34. Yuan, Y., Yang, H., and Li, C. Possible influences of the tropical Indian Ocean dipole on the eastward propagation of MJO. *Journal of Tropical Meteorology*, 2014, 20: 173-180.
35. Zhang, C. Madden-Julian Oscillation: Bridging weather and climate. *Bull. Amer. Meteor. Soc.*, 2013, 94: 1849-1870.
36. Zhang, L., N., Wang, B., Z., Zeng, C., Q. Impacts of the Madden-Julian oscillation on summer rainfall in Southeast China. *J., Climate*, 2009, 22: 201-216.